

Highlights

PSE-Net: Channel Pruning for Convolutional Neural Networks with Parallel-subnets Estimator

Shiguang Wang, Tao Xie, Haijun Liu, Xingcheng Zhang, Jian Cheng

- We propose PSE-Net, a novel parallel-subnets estimator for efficient channel pruning while evaluating the sampled subnets reliably. It's efficient and only needs 30%/16% total time compared with BCNet/AutoSlim for building the supernet estimator, respectively.
- We introduce the prior-distributed-based sampling algorithm, which facilitates the search of optimal subnets while resolving the challenge of discovering samples that fulfill resource constraints due to the long-tail distribution of network configuration.

PSE-Net: Channel Pruning for Convolutional Neural Networks with Parallel-subnets Estimator^{★,★★}

Shiguang Wang^a, Tao Xie^b, Haijun Liu^c, Xingcheng Zhang^d and Jian Cheng^{a,*}

^a University of Electronic Science and Technology of China, No.2006, Xiyuan Ave, West Hi-Tech Zone, Chengdu, 611731, China

^b Harbin Institute of Technology, Harbin, 150006, China

^c Chongqing University, Chongqing, 400044, China

^d Sensetime Research, Beijing, 100084, China

ARTICLE INFO

Keywords:

Channel Pruning
Neural Network Slimming
Network Pruning
Neural Architecture Search.

ABSTRACT

Channel Pruning is one of the most widespread techniques used to compress deep neural networks while maintaining their performances. Currently, a typical pruning algorithm leverages neural architecture search to directly find networks with a configurable width, the key step of which is to identify representative subnet for various pruning ratios by training a supernet. However, current methods mainly follow a serial training strategy to optimize supernet, which is very time-consuming. In this work, we introduce PSE-Net, a novel parallel-subnets estimator for efficient channel pruning. Specifically, we propose a parallel-subnets training algorithm that simulate the forward-backward pass of multiple subnets by dropping extraneous features on batch dimension, thus various subnets could be trained in one round. Our proposed algorithm facilitates the efficiency of supernet training and equips the network with the ability to interpolate the accuracy of unsampled subnets, enabling PSE-Net to effectively evaluate and rank the subnets. Over the trained supernet, we develop a prior-distributed-based sampling algorithm to boost the performance of classical evolutionary search. Such algorithm utilizes the prior information of supernet training phase to assist in the search of optimal subnets while tackling the challenge of discovering samples that satisfy resource constraints due to the long-tail distribution of network configuration. Extensive experiments demonstrate PSE-Net outperforms previous state-of-the-art channel pruning methods on the ImageNet dataset while retaining superior supernet training efficiency. For example, under 300M FLOPs constraint, our pruned MobileNetV2 achieves 75.2% Top-1 accuracy on ImageNet dataset, exceeding the original MobileNetV2 by 2.6 units while only cost 30%/16% times than BCNet/AutoAlim.

1. Introduction

Recently, Convolutional Neural Networks (CNNs) have evolved broader and achieved tremendous successes in various computer vision and machine learning applications, including image classification Krizhevsky, Sutskever and Hinton (2017); He, Zhang, Ren and Sun (2016), object detection Redmon, Divvala, Girshick and Farhadi (2016); Girshick (2015), semantic segmentation Lin, Milan, Shen and Reid (2017a); Long, Shelhamer and Darrell (2015), and action recognition Wang and Schmid (2013); Herath, Harandi and Porikli (2017). To enhance performance on these tasks, CNNs are becoming increasingly complex, with deeper and wider network designs. Nevertheless, deploying highly complex CNNs on modern devices with constrained resources, such as mobile devices, is impractical due to their excessive consumption of computational power and memory footprint. Many network compression approaches, including knowledge distillation Hinton, Vinyals, Dean et al. (2015), network pruning Guo, Wang, Li and Yan (2020a); Li, Adamczewski, Li, Gu, Timofte and Van Gool (2022); Zhao,

Zhang and Ni (2023); Kang (2019), quantization Rastegari, Ordonez, Redmon and Farhadi (2016), and matrix decomposition Wang, Hu, Fang, Zhao and Cheng (2017) have been proposed to minimize the storage expenses and computation of a single CNN while retaining its performance. Among these methods, network pruning has been the most popular technique due to its simple implementation and high pruning ratio with minimal performance loss.

Given an unpruned network, network pruning seeks to produce a leaner network capable of precise assessment and fast inference time. Early pruning researches focus mostly on reducing individual weights with a negligible effect on the performance of deep neural networks, often known as weight pruning Zhang, Ye, Zhang, Tang, Wen, Fardad and Wang (2018); Han, Pool, Tran and Dally (2015). Compared with weight pruning, channel pruning Guo et al. (2020a); Zhao et al. (2023); Chen, Liu, Yang, Li and Li (2022) is more straightforward since it eliminates the whole channel/filter rather than individual weights, making it possible to implement without the need for specialist software and hardware. Conventional channel pruning typically employs a pre-trained network and executes the pruning process end-to-end or layer-wisely. After pruning, it is deemed that a subnet with high accuracy is a plausible candidate for the ultimate solution.

Recently, it has been advocated that the key to channel pruning should be learning a more compact network configuration, i.e., width, in lieu of the retained weights Liu,

*This work was supported by the National Natural Science Foundation of China (No.62071104, No. U2233209, No. U2133211, and No. 62001063).

[★]Corresponding author

 xiaohu_wyyx@163.com (S. Wang); haijun_liu@126.com (H. Liu); zhangxingcheng@sensetime.com (X. Zhang); chengjian@uestc.edu.cn (J. Cheng)

ORCID(s):

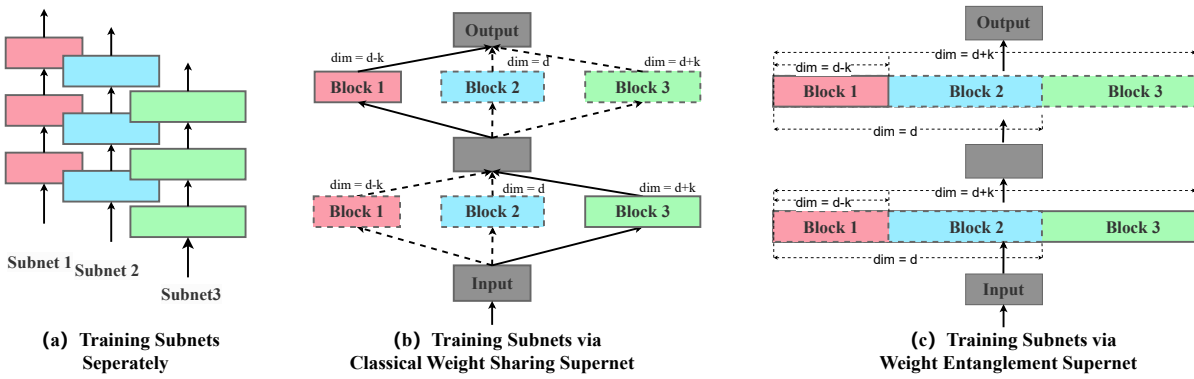


Figure 1: Different types of mechanisms for modeling estimator. (a). Thousands of distinct models are trained separately. (b) and (c) are two types of weight-sharing supernet mechanisms adopted by most one-shot NAS methods. Suppose we have three blocks with $d - k$, d , and $d + k$ channels, separately, the classical weight-sharing supernet (b) will separately build weights for these blocks, while the weight entanglement supernet will entangle these blocks with super weights. We denote the chosen parts in solid lines while the unchosen parts are in dashed lines. One-shot NAS methods like SPOS Guo et al. (2020b), FairNAS Chu et al. (2021), Cream Peng et al. (2020) adopt the modeling mechanism (b), while AutoSlim Yu and Huang (2019a), BigNAS Yu et al. (2020), BCNet Su et al. (2021), and Ours adopt the modeling mechanism (c).

Sun, Zhou, Huang and Darrell. In this way, the quantity of filters or channels is utilized as a direct indicator of network width. Thus, subsequent researches employ neural architecture search (NAS) or other AutoML methods, including MetaPruning Liu, Mu, Zhang, Guo, Yang, Cheng and Sun (2019), AutoSlim Yu and Huang (2019a), and TAS Dong and Yang (2019), to directly identify the optimal network configuration. Typically, these methods entail three steps: (1) optimizing a **estimator** (i.e., **supernet**) over a number of epochs to effectively derive a benchmark performance estimator; (2) iteratively evaluating the trained supernet and obtaining the optimized **channel configurations** (i.e., **subnet**) under various resource constraints with minimal accuracy drop on the validation set; and (3) and retraining these optimized architectures from scratch under full training epochs.

The most critical step of AutoML methods for channel pruning is training the benchmark performance estimator for evaluating various subnets. Theoretically, a decent estimator should adhere to two principle rules: (1) effectively identifying representative subnets under resource constraints and (2) efficiently evaluating different subnets. Customarily, one-shot NAS Guo et al. (2020b); Peng et al. (2020) approaches have been used to train the estimator (i.e., supernet) due to their low computational overhead and competitive performance. As shown in Fig. 1, instead of training thousands of distinct models from scratch (Fig. 1 (a)), one-shot approaches just train a single massive supernet (Fig. 1 (b) and Fig. 1 (c)), i.e., a performance estimator that can emulate any architectures in the search space, with weights shared among architectural candidates. Consequently, the performance of a network channel configuration refers to the precision of the defined subnet with shared supernet weights.

However, sharing a single set of weights cannot ensure that each subnet receives sufficient training, hence diminishing the reliability of evaluating subnets. BCNet Su et al. (2021) characterizes such unreliability as unequal training

periods for each channel in the convolution layer and proposes a new estimator, namely Bilaterally Coupled Network, to alleviate the training and assessment inequities. Nonetheless, the fairness of *channel-level* training cannot fully reflect the corresponding *network-level* training. In addition, BCNet is inefficient for training supernet as the training batch must be forwarded and backwarded twice at each training iteration. Alternatively, other approaches such as BigNAS Yu et al. (2020) and AutoSlim Yu and Huang (2019a) think about sufficient training from *network-level*, which sample multiple subnets to execute forward-backward serially and aggregate the gradients from all sampled subnets before updating the weights of the supernet. It helps to provide more interpretive information by making the performance boundary of the search space available in validation, thereby improving the reliability of assessing subnets. However, such a process is roughly equivalent to training a plain model multiple times and thus slows the training efficiency of the supernet.

In this work, we introduce PSE-Net, a novel parallel-subnets estimator for efficient channel pruning. Specifically, we follow the *network-level* design paradigm that sampling multiple subnets for supernet updating at each iteration. To facilitate the supernet training, we propose the **parallel-subnets training algorithm**, a supernet training technique that focuses on time-efficient training by holding the supernet and dropping unnecessary features on batch dimension to simulate the forward-backward of multiple sampled subnets in one round. The parallel-subnets training algorithm enables the forward-backward execution of multiple networks in parallel, hence improving the training efficiency of the supernet while arming the network with the capability of interpolating the accuracy of unsampled subnets. In this way, after training, it is possible for PSE-Net to evaluate the performance of the sampled subnets reliably. As for the subsequent searching, we introduce the **prior-distributed-based sampling algorithm**, which draws architecture samples for

performance accessing according to the prior distribution. The **prior distribution** is efficiently estimated by utilizing the training loss and computation cost (e.g., FLOPs) of various subnets during supernet training. In which the training loss reflect the quality of each subnet while the computation cost represent the resource constraints. Thus, to sample a random subnet subject to a FLOPs restriction, we directly employ rejection sampling from the prior distribution, which offers a significantly higher sampling efficiency and samping quality than directly sampling from the entire search space.

To summarize, the main contributions of this work are as follows:

- We propose PSE-Net, a novel parallel-subnets estimator for efficient channel pruning while evaluating the sampled subnets reliably. It's efficient and only needs 30%/16% total time compared with BCNet/AutoSlim for building the supernet estimator, respectively.
- We introduce the prior-distributed-based sampling algorithm, which facilitates the search of optimal subnets while resolving the challenge of discovering samples that fulfill resource constraints due to the long-tail distribution of network configuration.
- Comprehensive experiments on the ImageNet benchmark and downstream datasets indicate that our approach efficiently exceeds the SOTAs for a variety of FLOPs budgets.

2. Related works

Network pruning techniques can be broadly categorized into two types, i.e., non-structured pruning and structured pruning. Non-structured pruning removes individual weights from the network, leading to a sparse weight matrix. However, this sparsity cannot be fully exploited in all the hardware implementations, thereby limiting the acceleration of the pruned network. In comparison, structured pruning (i.e., channel pruning) removes whole filters, resulting in structure sparsity. This work is based on channel pruning and will sort out related works from the following two aspects.

2.1. Criterion Based Channel Pruning

Numerous pruning techniques have been proposed to evaluate the importance of filters or channels in convolutional neural networks (CNNs). Some approaches define specific criteria for assessing channel significance. For instance, Li, Kadav, Durdanovic, Samet and Graf; He, Kang, Dong, Fu and Yang (2018a) advocate for the use of the l_1 -norm as a channel ordering criterion. In a different vein, Hu, Peng, Tai and Tang (2016) prunes channels based on a lower average proportion of zeros (APoZ) after ReLU activation. Another strategy by Molchanov, Tyree, Karras, Aila and Kautz involves approximating the change in the loss function through Taylor expansion, where channels causing the least change in the loss function are considered less significant. Meanwhile, Luo, Wu and Lin (2017) prunes filters based on statistical data from the subsequent layer, and He, Liu,

Wang, Hu and Yang (2019) computes the geometric average of filters within the same layer, excluding those closest to the average. Lin, Ji, Wang, Zhang, Zhang, Tian and Shao (2020) suggests eliminating channels with low-rank feature maps, while He, Ding, Liu, Zhu, Zhang and Yang (2020) employs diverse metrics to gauge the significance of filters across layers. The GlobalPru, proposed by Pan, Yang, Foo, Ke, Rahmani, Fan and Liu (2023) propose a channel attention-based learn-to rank framework to learn a global ranking of channels with respect to network redundancy.

These methods metrics-based prioritize the selection of "important" filters over discovering optimal channel topologies. Despite the achievements, the majority of these methods specify pruning proportions or hyperparameters in a hand-craft manner, which is complex, time-consuming, and makes it tough to identify optimal solutions.

2.2. Search Based Channel Pruning

Inspired by the advancements in neural architecture search (NAS) techniques Guo et al. (2020b); Yu and Huang (2019b); Yu et al. (2020), recent works resort to leveraging the NAS to identify optimal channel configurations. In He, Lin, Liu, Wang, Li and Han (2018b), reinforcement learning is employed for layer-wise exploration of channel numbers. Taking inspiration from curriculum learning, Camci, Gupta, Wu and Lin (2022) tailors pruning strategies for each sparsity level based on their complexity. Liu et al. (2019) and Yu and Huang (2019a) firstly train a one-shot supernet and then seek efficient architectures inside it. Dong and Yang (2019) introduces a differentiable NAS approach that can efficiently search transformable networks with variable width and depth. Lin, Ji, Zhang, Zhang, Wu and Tian (2021) provides a new approach for channel pruning based on the artificial bee colony algorithm (ABC), named ABCPruner, which seeks to identify optimal pruned structures in an efficient manner. Characterizing channel pruning as a Markov process, Guo et al. (2020a) enables differentiable channel pruning. Tackling biases in network width search, BCNetSu et al. (2021) establishes a new estimator to alleviate training and assessment biases.

In either the process of training a large one-shot supernet or the process of searching for an ideal design, these approaches incur a substantial computational cost. To offer a efficient and reliable performance estimator, our proposed PSE-Net focuses on time-efficient training by holding the supernet and dropping unnecessary features on batch dimension to simulate multiple sampled subnets forward-backward in one round.

3. Method

We introduce our proposed method starting from the discussion of neural architecture search for channel pruning. Then, we will give the details of the proposed parallel-subnets training algorithm for efficient supernet training. Next, we introduce our prior-distributed-based sampling algorithm for efficient yet effective evolutional searching. Finally, we illustrate how to embed the proposed techniques

into the pruning pipeline. The overall framework is illustrated in Fig. 2.

3.1. Neural Architecture Search for Channel Pruning

Given an unpruned network \mathcal{N} , containing L layers (e.g., convolutional layers and normalization layers), we can represent the architecture of \mathcal{N} as $\mathcal{A} = \{C_1, C_2, \dots, C_l, \dots, C_L\}$, where C_l is the output channel number of the l -th layer. Then, the objective of channel pruning is to layer-wisely make out redundant channels (indexed by \mathcal{T}_l^{pruned}), i.e., $\mathcal{T}_l^{pruned} \subset [1, C_l]$, where $[1, C_l]$ is an index set for all integers in the range of 1 to C_l for the l -th layer.

However, recent empirical research by Liu et al. demonstrates that the absolute set of pruned channels \mathcal{T}_l^{pruned} and their weights are not essential for the performance of a pruned network, but the resultant width C'_l of each layer is significant, i.e.,

$$C'_l = C_l - |\mathcal{T}_l^{pruned}|. \quad (1)$$

In this manner, recently popular AutoML-based structured pruning approaches view channel pruning as an automatic channel search with the **search space** \mathcal{A} amounts to $|\mathcal{A}| = \prod_{l=1}^L C_l$, e.g., 20^{50} for $L = 50$ layers and $C_l = 20$ channels. To reduce the search space, current methods tend to search at the group level rather than the channel level. Specifically, all channels at a layer are equally partitioned into K groups, then we only need to consider K cases: there are just $(C_l/K) \cdot [1 : K]$ layer width choices for the l -th layer. As a result, the search space is shrunk into K^L . Then, using neural architecture search (NAS) for channel pruning involves two phases:

Constraint-free Pre-training (phase 1): In this phase, we target learning the parameters of the weight-sharing supernet, i.e., the performance estimator. Specifically, the weights \mathcal{W} of the target supernet \mathcal{N} is trained by uniformly sampling a width \mathcal{A}' and optimizing its corresponding subnet with weights $\mathcal{W}_{\mathcal{A}'} \subset \mathcal{W}$:

$$\mathcal{W}^* = \min_{\mathcal{W}_{\mathcal{A}'} \in \mathcal{W}} \mathcal{L}_{trn}(\mathcal{A}', \mathcal{W}_{\mathcal{A}'}; \mathcal{N}, \mathcal{D}_{trn}), \quad (2)$$

where $\mathcal{L}_{trn}(\cdot)$ is the training loss function, \mathcal{D}_{trn} represents the training dataset, and \mathcal{W}^* denotes the trained weights.

Resource-constrained Searching (phase 2): After the pre-training in phase 1, the optimal network width \mathcal{A}^* corresponds to the one with the best performance on the validation dataset under the constraint resources, e.g., classification accuracy,

$$\begin{aligned} \mathcal{A}^* = & \arg \max_{\mathcal{A}' \in \mathcal{A}} \text{Accuracy}(\mathcal{A}', \mathcal{W}_{\mathcal{A}'}; \mathcal{W}, \mathcal{N}, \mathcal{D}_{val}), \\ & \text{s.t. } \text{Cons}(\mathcal{N}_{pruned}(\mathcal{A}', \mathcal{W}')) < \epsilon \end{aligned} \quad (3)$$

where \mathcal{D}_{val} denotes the validation dataset, $\text{Cons}(\cdot)$ is the proxy function for computational cost, ϵ is a specified budget of constraint resource. The searching process for Eq. (3) can

be performed efficiently by various algorithms, such as random search or evolutionary search. Then, the performance of the searched optimal width \mathcal{A}^* is analyzed by training from scratch.

The weight sharing strategy in **phase 1** reduces the search cost by several orders of magnitude. However, it still poses a potential problem, i.e., the insufficient training of subnets within the supernet. Due to such an issue, there is a limited correlation between the performance of an architecture measured by the one-shot weight and its actual performance. Therefore, the search based on the weight \mathcal{W} may not uncover promising architectures, producing a less than ideal solution. Towards this end, some methods Yu et al. (2020); Yu, Yang, Xu, Yang and Huang replace Eq. (2) with following optimization problem:

$$\mathcal{W}^* = \min_{\mathcal{W}} \mathbb{E}_{\mathcal{A}' \in \mathcal{A}} [\mathcal{L}_{trn}(\mathcal{A}', \mathcal{W}_{\mathcal{A}'}; \mathcal{N}, \mathcal{D}_{trn})] + \gamma \mathcal{R}(\mathcal{W}), \quad (4)$$

where $\mathcal{R}(\mathcal{W})$ is the regularization term, and $\mathbb{E}[\cdot]$ denotes the expectation of random variables.

In practice, the expectation term in Eq. (4) is usually approximated by n uniformly sampled architectures and solved by SGD optimization algorithm, formulated as:

$$\mathcal{W}^* = \min_{\mathcal{W}} \sum_{i=1}^n \mathcal{L}_{trn}(\mathcal{A}'_i, \mathcal{W}_{\mathcal{A}'_i}; \mathcal{N}, \mathcal{D}_{trn}). \quad (5)$$

Nevertheless, **such serial training strategy requires to execute forward-backward n times and aggregate the gradients from all sampled models at each training iteration, which is approximately equal to training a plain model n times, thus slowing the training efficiency of the supernet, as illustrated in Fig. 2 (a)**. Thus, we propose parallel-subnets training algorithm that enables multiple networks to be executed forward-backward in parallel, improving the training efficiency of the supernet while arming the network with the capability of interpolating the accuracy of unsampled subnets.

3.2. From Serial Training Strategy to Parallel-subnets Training Algorithm

For the l -th layer of \mathcal{N} , we define its weight as $w_l \in \mathbb{R}^{C_l \times C_{l-1} \times \mathcal{K}_l}$, where \mathcal{K}_l is additional dimensions of the layer. The input feature maps of the l -th layer are denoted by $\mathcal{I}_l = \{\mathcal{I}_l^1, \mathcal{I}_l^2, \dots, \mathcal{I}_l^p, \dots, \mathcal{I}_l^{C_{l-1}}\} \in \mathbb{R}^{b \times C_{l-1} \times h_{l-1} \times w_{l-1}}$, where b is the batch size of the input, and h_{l-1} and w_{l-1} are the height and width, respectively. For convenient portrayal, we denote the collection of weights connected to the q -th output channel as $w_l^{q,:}$, and the collection of weights connected to the p -th input channel as $w_l^{:p}$. The p -th input feature map \mathcal{I}_l^p is connected to $w_l^{:p}$ of the layer to generate the output feature map. The general operation of the l -th layer can be then defined as follows:

$$\mathcal{F}_l(\mathcal{I}_l) = \sum_{p=1}^{C_{l-1}} \mathcal{I}_l^p * w_l^{:p}, \quad (6)$$

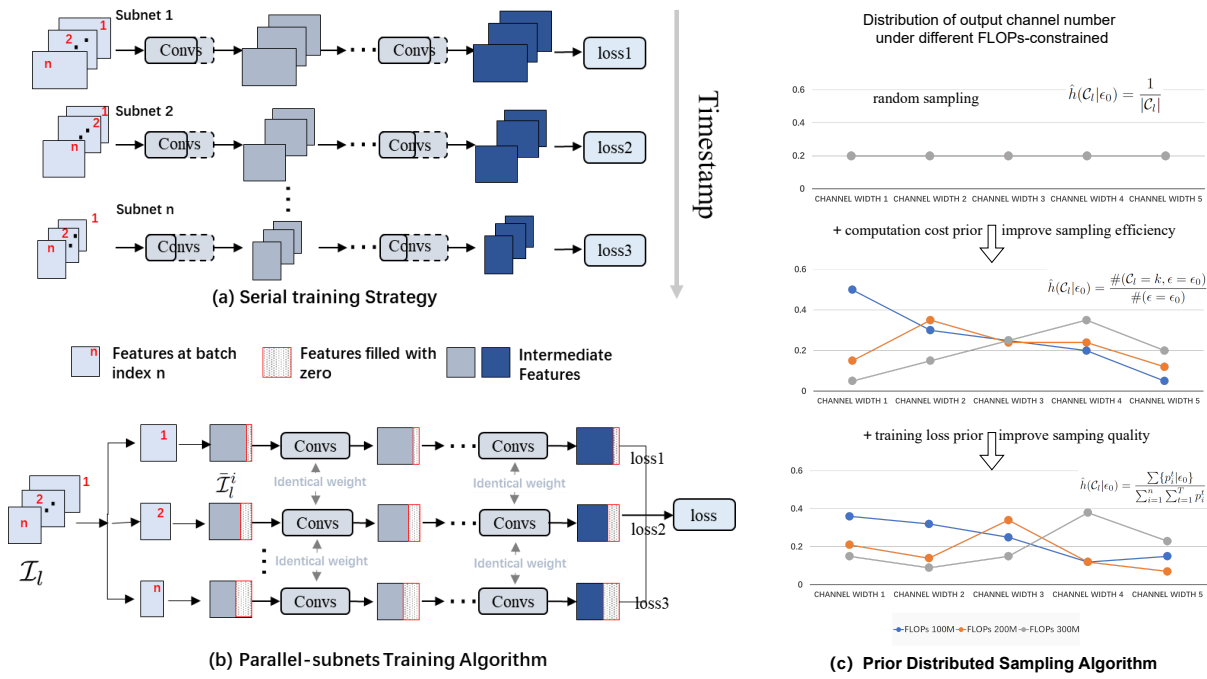


Figure 2: The overall framework of PSE-Net. We propose a parallel-subnets training algorithm and prior-distributed-based sampling algorithm to boost supernet training and subnet searching, respectively. Comparison of serial training strategy and parallel-subnets training algorithm during the supernet training phase is illustrated in (a) and (b). (a) Serial training strategy is approximately equal to training a plain model n times, thus slowing the training efficiency of the supernet. (b) Parallel-subnets training algorithm that always holds the supernet and drops extraneous features on batch dimension to simulate multiple subnets forward-backward in one round. We denote the chosen parts in solid lines while the unchosen parts are in dashed lines. (c) Apart from introducing the computation cost for improving sampling efficiency, we also adopt the training loss that reflecting the quality of subnets to improve subnet sampling performance.

where $*$ denotes the basic operator in CNN, such as 2D convolution and batch normalization.

During the pruning process, given the input feature $\mathcal{I}_l = \{\mathcal{I}_l^1, \mathcal{I}_l^2, \dots, \mathcal{I}_l^p, \dots, \mathcal{I}_l^{C'_{l-1}}\} \in \mathbb{R}^{b \times C'_{l-1} \times h_{l-1} \times w_{l-1}}$, where $C'_{l-1} \leq C_{l-1}$ is the pruned output channel of the $(l-1)$ -th layer, each p -th feature map \mathcal{I}_l^p has the same dimension with the others. In this way, for the l -th layer in the model \mathcal{N} , Eq. (6) can be expressed sequentially as the following formula:

$$\left\{ \begin{array}{l} \mathcal{Y}^{q_1} = \mathcal{F}_l^{q_1}(\mathcal{I}_l) = \sum_{p=1}^{C'_{l-1}} \mathcal{I}_l^p * w_l^{:q_1,p} \\ \mathcal{Y}^{q_2} = \mathcal{F}_l^{q_2}(\mathcal{I}_l) = \sum_{p=1}^{C'_{l-1}} \mathcal{I}_l^p * w_l^{:q_2,p} \\ \mathcal{Y}^{q_i} = \mathcal{F}_l^{q_i}(\mathcal{I}_l) = \sum_{p=1}^{C'_{l-1}} \mathcal{I}_l^p * w_l^{:q_i,p} \\ \mathcal{Y}^{q_n} = \mathcal{F}_l^{q_n}(\mathcal{I}_l) = \sum_{p=1}^{C'_{l-1}} \mathcal{I}_l^p * w_l^{:q_n,p}, \end{array} \right. \quad (7)$$

where $q_i, i = 1, 2, \dots, n$ denotes the i -th random sampled output channel from the predefined search space, $\mathcal{Y}^{q_i} \in \mathbb{R}^{b \times C_l^{q_i} \times h_l \times w_l}$ is the output feature by input features and the first q_i channel weights, i.e., $w_l^{:q_i,p}$.

Such naive training enables the simple training of numerous networks inside a single architecture without compromising performance. It helps to display more interpretive information by rendering the performance boundary of the search space accessible during validation. However, in each

iteration, due to the different size of $w_l^{:q_i,p}$ in each subnet, n subnets must run serially by taking the same input feature \mathcal{I}_l as input, and then aggregate their gradients, which impacts the training efficiency of the supernet. Theoretically, it would slow down the training process n times. Towards this end, **we propose a parallel-subnets training algorithm that leverages the largest network as the forward-backward proxy and simulates multiple sampled subnets along the batch dimension in one round, thereby accelerating the supernet training**, as shown in Fig. 2 (b). Specifically, we divide the input \mathcal{I}_l into n parts along the batch dimension, which is formulated as follows:

$$\mathcal{I}_l = [\mathcal{I}_l^1, \mathcal{I}_l^2, \dots, \mathcal{I}_l^i, \dots, \mathcal{I}_l^n], \quad (8)$$

where $\mathcal{I}_l^i \in \mathbb{R}^{b \times C'_{l-1} \times h_{l-1} \times w_{l-1}}$ is the i -th part of \mathcal{I}_l , where each part corresponds to a subnet, respectively.

For the i -th part $\mathcal{I}_l^i = \{\mathcal{I}_l^{1,i}, \mathcal{I}_l^{2,i}, \dots, \mathcal{I}_l^{C'_{l-1},i}\} \in \mathbb{R}^{b \times C'_{l-1} \times h_{l-1} \times w_{l-1}}$ of \mathcal{I}_l , we pad \mathcal{I}_l^i to $\bar{\mathcal{I}}_l^i$ with 0 along the channel dimension so that it can be fed into the largest layer (the layer with the largest output channel):

$$\bar{\mathcal{I}}_l^i = [\mathcal{I}_l^i, 0] = \{\mathcal{I}_l^{1,i}, \mathcal{I}_l^{2,i}, \dots, \mathcal{I}_l^{C'_{l-1},i}, 0\}, \quad (9)$$

where $\bar{\mathcal{I}}_l^i \in \mathbb{R}^{b \times C_{l-1} \times h_{l-1} \times w_{l-1}}$ is leveraged as the input of the largest layer. In this way, we can transform $\bar{\mathcal{I}}_l^i$ to

the intermediate feature by using the largest layer, which is formulated as:

$$\bar{\mathcal{Y}}^i = \mathcal{F}_l(\bar{\mathcal{I}}_l^i) = \sum_{p=1}^{C_{l-1}} \bar{\mathcal{I}}_l^{p,i} * w_l^{i,p}, \quad (10)$$

where $\bar{\mathcal{Y}}^i \in \mathbb{R}^{\frac{b}{n} \times C_l \times h_l \times w_l}$ is the output of the largest layer C_l .

However, the $\bar{\mathcal{Y}}^i \in \mathbb{R}^{\frac{b}{n} \times C_l \times h_l \times w_l}$ is not approximate to $\mathcal{Y}^{q_i} \in \mathbb{R}^{b \times C_l^{q_i} \times h_l \times w_l}$ along the channel dimension. Supposing a function $\mathcal{G}(\cdot)$ that applies to $\bar{\mathcal{Y}}^i$, we can get \mathcal{Y}^{q_i} through transformation:

$$\mathcal{Y}^{q_i} \propto \mathcal{G}(\bar{\mathcal{Y}}^i), \quad (11)$$

Thus, by feeding $\bar{\mathcal{I}}_l^i, i = 1, 2, \dots, n$ into the largest convolutional layer at once, we get \mathcal{Y} in one run as follows:

$$\mathcal{Y} = \mathcal{G}(\sum_{p=1}^{C_{l-1}} [\bar{\mathcal{I}}_l^{p,1}, \bar{\mathcal{I}}_l^{p,2}, \dots, \bar{\mathcal{I}}_l^{p,i}, \dots, \bar{\mathcal{I}}_l^{p,n}] * w_l^{i,p}), \quad (12)$$

where $\mathcal{Y} = [\bar{\mathcal{Y}}^1, \bar{\mathcal{Y}}^2, \dots, \bar{\mathcal{Y}}^n]$ equals $[\mathcal{Y}^{q_1}, \mathcal{Y}^{q_2}, \dots, \mathcal{Y}^{q_n}]$ in the batch dimension if feeding the same data. In this manner, we are capable of imitating the concurrent training of many subnets in each mini-batch, enabling the network to interpolate the accuracy of unsampled subnets. As such, it is possible to assess the performance of the sampled subnets in a reliable way after training. Next we derive the corresponding function $\mathcal{G}(\cdot)$ according to the common functions.

Convolution. We define a mask matrix \mathcal{M}^i to enable $\bar{\mathcal{Y}}^i$ to approximate \mathcal{Y}^{q_i} along the channel dimension so that the performance boundary of the search space is accessible during validation. Based on the linear property of convolution, we can get the (j, k) -th component of the mask matrix \mathcal{M}^i as follows:

$$\mathcal{M}_{jk}^i = \begin{cases} 1 & \text{if } \frac{b}{n} \times i \leq j < \frac{b}{n} \times (i+1), k \leq C_l^{q_i}, \\ 0 & \text{otherwise} \end{cases} \quad (13)$$

where $C_l^{q_i}$ is the random sampled output channel of the l -th convolutional layer.

Therefore, the function $\mathcal{G}(\cdot)$ for convolutional layer is element-wise product, which is formulated as:

$$\mathcal{Y}^{q_i} \propto \mathcal{M}^i \otimes \bar{\mathcal{Y}}^i, \quad (14)$$

where \otimes is element-wise product. The linear layer can be viewed as a convolution layer with a convolution kernel of 1 and a stride of 1, hence its mask matrix is identical to that of the convolutional layer.

Batch Normalization. Typically, we often add a batch normalization layer after the convolution layer to expedite network training. Given the input feature \mathcal{I}_l , the pair of parameters γ and β scale and shift the normalized value as: $\gamma \mathcal{I}_l + \beta$. These parameters are learned along with the original model parameters, and restore the representation capacity of the network. Based on this observation, we can see that batch

normalization layer also has linear property. In this way, the function $\mathcal{G}(\cdot)$ has a same form with Eq. (13) and Eq. (14).

Notably, batch norm statistics are not accumulated when training the supernet model, since they are ill-defined with varying architectures in parallel-subnets training algorithm. The batch norm statistics are re-calibrated after the training is completed, which is memory efficient and effective in handling weight-entanglement supernet training.

3.3. Searching Subnet with Prior-Distributed-Based Sampling Algorithm

After the supernet \mathcal{N} has been trained with \mathcal{W}^* , each channel configuration \mathcal{A}' can be evaluated by estimating its performance (e.g., classification accuracy) on the validation dataset \mathcal{D}_{val} using the Eq. (3). One of which critical steps entails drawing architecture examples according to diverse resource restrictions (e.g., FLOPs in this work). At each sampling step, it's necessary to first select a sample of target FLOPs ϵ . Due to the inability of enumerating all evaluable structures, previous researchers resort to random search, evolutional search, and reinforcement learning to find the most promising architecture. However, **it may be hard to find samples that meet resource constraints, due to the long-tail distribution of network configuration**. On the other hand, a network configuration that performs well on the training set also has a greater chance of performing better on the validation set. If we collect prior information during the training of a supernet to construct a distribution, we can sample a network with superior performance more efficiently.

Towards this end, we propose a novel search algorithm for promising architecture search in an efficient way. Specifically, we propose to approximate $h(\mathcal{A}|\epsilon_0)$ empirically to accelerate the FLOPs-constrained sampling procedure, where $h(\mathcal{A}|\epsilon_0)$ is the distribution over architectures conditioned on constraint ϵ_0 . As illustrated in Section 3.2, the supernet has a set of L convolutional layers $\mathcal{A} = \{C_1, C_2, \dots, C_l, \dots, C_L\}$, where C_l denotes the output channel number of the l -th layer. Let $\hat{h}(\mathcal{A}|\epsilon_0)$ denote an empirical approximation of $h(\mathcal{A}|\epsilon_0)$, for simplicity, we relax,

$$\hat{h}(\mathcal{A}|\epsilon_0) \propto \prod_{l=1}^L \hat{h}(C_l|\epsilon_0). \quad (15)$$

Let $\#(C_l = k, \epsilon = \epsilon_0)$ be the number of times that the pair $(C_l = k, \epsilon = \epsilon_0)$ occurs in the sample pool of architecture-FLOPs. Thus, a straightforward method to approximate $\hat{h}(C_l|\epsilon_0)$ is formulated as:

$$\hat{h}(C_l|\epsilon_0) = \frac{\#(C_l = k, \epsilon = \epsilon_0)}{\#(\epsilon = \epsilon_0)}. \quad (16)$$

However, **such a naive way does not consider the subnet quality during sampling, which can be reflected by the prior information during supernet training**.

More specifically, as illustrated in Fig. 2 c, during the supernet training, we sample various widths to generate

subnets at each iteration, the quality of which can be measured by the training loss. Thus, we can capture numerous subnets with associated training loss and training iterations during supernet training. Notably, as our supernet forwards n subnets in parallel at each iteration, we can acquire a loss collection of n distinct subnets during each iteration, which is formulated as:

$$\mathcal{L}^t = \{\mathcal{L}_{trn}(\mathcal{W}_{\mathcal{A}_i^t}; \mathcal{A}_i^t)\}_{i=1}^n, \quad (17)$$

where \mathcal{A}_i^t is the i -th sampled channel configuration at the t -th iteration during supernet training.

Suppose we train the supernet T iterations. As a result, we can get the total loss collection at the end training of supernet:

$$\mathcal{L} = \{\mathcal{L}^1, \mathcal{L}^2, \dots, \mathcal{L}^t, \dots, \mathcal{L}^T\}. \quad (18)$$

Nevertheless, since the weight \mathcal{W} of supernet is continuously updated, using the loss record over various iterations cannot accurately reflect the real potential of the corresponding channel configuration. Thus, we define proxy loss for each configuration as follows:

$$p_i^t = \frac{\mathcal{L}_{trn}(\mathcal{W}_{\mathcal{A}_{max}^t}; \mathcal{A}_{max}^t)}{\mathcal{L}_{trn}(\mathcal{W}_{\mathcal{A}_{max}^T}; \mathcal{A}_{max}^T)} \mathcal{L}_{trn}(\mathcal{W}_{\mathcal{A}_i^t}; \mathcal{A}_i^t), \quad (19)$$

where \mathcal{A}_{max}^t is the largest subnet of the supernet, with $\mathcal{A}_{max}^t = \mathcal{A}_{max}^1 = \mathcal{A}_{max}^2 = \dots = \mathcal{A}_{max}^T$.

Therefore, the empirical approximation of $\hat{h}(\mathcal{C}_l | \epsilon_0)$ can be estimated as:

$$\hat{h}(\mathcal{C}_l | \epsilon_0) = \frac{\sum \{p_i^t | \epsilon_0\}}{\sum_{i=1}^n \sum_{t=1}^T p_i^t}, \quad (20)$$

where $\{p_i^t | \epsilon_0\}$ is the architecture collections that yield FLOPs ϵ_0 .

3.4. Pruning Pipeline

SuperNet Training. Since the whole unpruned network is composed of convolution layers, normalization layers, and activation layers, all of which possess linear properties, the unpruned network also retains linear properties, allowing our suggested parallel-subnets training algorithm to be applied layer-by-layer to the network. At each training iteration, we forward the supernet and drop unnecessary features along the batch dimension to simulate the forward-backward pass of multiple subnets in one round, thereby accelerating the training of the supernet and equipping it with the ability to interpolate the accuracy of unsampled subnets.

It is worth noting that this does not require more GPU resources, as all one-shot NAS-based pruning algorithms require storing the entire supernet in memory. As for the computing memory overhead, other algorithms may also sample the largest subnet during the training process, and our algorithm always holds the supernet and drops extraneous features on batch dimension to simulate multiple subnets, so

the maximum computational memory consumption is also the same.

Prior-Distributed-Based Evolution Search. Over the trained supernet, we perform a prior-distributed-based evolution search to obtain the optimal subnets (channel configurations) under resource constraints. At the beginning of the search, we pick $\frac{P}{2}$ architectures with the top p_i^t and $\frac{P}{2}$ random architectures from the distribution $\hat{h}(\mathcal{A} | \epsilon_0)$ as seeds. The top k architectures are chosen as parents for generating the next offspring by mutation and crossover. At each generation of a crossover, two randomly selected candidates are crossed to produce a new individual. If the number of offspring produced by crossover and mutation is insufficient, we sample the architecture directly from $\hat{h}(\mathcal{A} | \epsilon_0)$.

Subnet Retrain. After obtaining the optimal subnets under resource constraints, we retrain them from scratch to derive their true performance.

4. Experimental Results

In this section, we conduct extensive experiments on the ImageNet dataset with various network architectures, e.g., ResNet50 He et al. (2016), MobileNetV2 Sandler, Howard, Zhu, Zhmoginov and Chen (2018) and VGG Simonyan and Zisserman (2014), to validate the efficacy of our PSE-Net.

4.1. Implementation Details

Search Space. For ResNet50/VGG, the original model is considered as the unpruned network for all models and the channels of each layer are partitioned into $K=10/20$ groups. For MobileNetV2, we consider two types of unpruned networks: the original model ($1\times$ FLOPs) and a modified version with $1.5\times$ FLOPs achieved through constant width scaling. The channels of each layer are partitioned into $K=20$ groups. We maintain a maximum pruning rate of 80% per layer to ensure that the network performance does not degrade.

SuperNet Training. For ResNet50, the training recipe is set as: LAMB optimizer with weight decay 2e-2, initial learning rate 0.008, 120 training epochs in total. For MobileNetV2, the training recipe is set as: SGD optimizer with momentum 0.9, nesterov acceleration, weight decay 4e-5, and 90 training epochs in total. The initial learning rate for training supernet is first warming up from 0 to 0.8 within 4 epochs, then is reduced to 0 by cosine scheduler. For VGG, the training recipe is set as: SGD optimizer with momentum 0.9, weight decay 1e-4, the initial learning rate 0.1 decayed by 10x at the 30-th, 60-th and 90-th epoch, 100 training epochs in total. For all our experiments, we split the input into $n=4$ parts and simulate multiple networks (one largest subnet and three random middle subnets) to execute forward-backward pass in one round at each training iteration.

Pruned Subnet Searching. The implementation of pruned subnet searching follows most protocols of evolution search in SPOS Guo et al. (2020b). We set the number of seeds P to 128, k to 64, and mutation probability to 0.2.

Table 1

Performance comparison of ResNet50 He et al. (2016) under ImageNet dataset. Performances are evaluated by using a single scale of 224×224. FLOPs is computed under the input resolution of 224×224. #Params denotes the number of parameters. Methods marked with “*” denote that reporting the results with knowledge distillation. † means the results reported in BCNet Su et al. (2021).

ResNet50						
FLOPs	Methods	FLOPs	#Params	Top-1	Top-5	
3G	Uniform [†]	3.0G	19.1M	75.9%	93.0%	
	Random [†]	3.0G	-	75.2%	92.5%	
	AutoSlim* Yu and Huang (2019a)	3.0G	23.1M	76.0%	-	
	LEGR Chin, Ding, Zhang and Marculescu (2019)	3.0G	-	76.2%	-	
	MetaPruning Liu et al. (2019) <i>cvpr19</i>	3.0G	-	76.2%	-	
	BCNet Su et al. (2021) <i>cvpr21</i>	3.0G	22.6M	77.3%	93.7%	
	PEEL Hou, Ma, Liu, Wang and Loy (2024) <i>pr24</i>	3.0G	-	76.6%	-	
2G	PSE-Net	3.0G	21.5M	77.9%	93.7%	
	Uniform [†]	2.0G	13.3M	75.1%	92.7%	
	Random [†]	2.0G	-	74.6%	92.2%	
	SSS Huang and Wang (2018) <i>eccv18</i>	2.8G	-	74.2%	91.9%	
	GBN You, Yan, Ye, Ma and Wang (2019) <i>NeurIPS19</i>	2.4G	31.83M	76.2%	92.8%	
	TAS* Dong and Yang (2019) <i>NeurIPS19</i>	2.3G	-	76.2%	93.1%	
	AutoSlim* Yu and Huang (2019a)	2.0G	20.6M	75.6%	-	
	LEGR Chin et al. (2019)	2.4G	-	75.7%	92.7%	
	PGPM He et al. (2019) <i>cvpr19</i>	2.4G	-	75.6%	92.6%	
	MetaPruning Liu et al. (2019) <i>cvpr19</i>	2.0G	-	75.4%	-	
	DMCP Guo et al. (2020a) <i>cvpr20</i>	2.2G	-	76.2%	-	
	BCNet Su et al. (2021) <i>cvpr21</i>	2.0G	18.4M	76.9%	93.3%	
	Tukan et al. Tukan, Mualem and Maalouf (2022) <i>NeurIPS22</i>	2.0G	-	75.1%	-	
	SANP Gao, Zhang, Zhang, Huang and Huang (2023) <i>iccv23</i>	1.9G	-	76.7%	-	
1G	Roy et al. Miles and Mikolajczyk (2023) <i>iccv23</i>	1.9G	-	75.6%	-	
	PEEL Hou et al. (2024) <i>pr24</i>	2.2G	-	76.5%	-	
	ARPruning Yuan, Li, Liu, Tang and Liu (2024) <i>nn24</i>	1.8G	11.0M	72.3%	-	
	PSE-Net	2.0G	18.0M	77.3%	93.4%	
	Uniform [†]	1.0G	6.9G	73.1%	91.8%	
	Random [†]	1.0G	-	72.2%	91.4%	
	AutoSlim* Yu and Huang (2019a)	1.0G	13.3M	74.0%	-	
100M	MetaPruning Liu et al. (2019) <i>cvpr19</i>	1.0G	-	73.4%	-	
	AutoPruner Luo and Wu (2020) <i>pr20</i>	1.4G	-	73.1%	91.3%	
	BCNet Su et al. (2021) <i>cvpr21</i>	1.0G	12M	75.2%	92.6%	
	PEEL Hou et al. (2024) <i>pr24</i>	1.1G	-	74.7%	-	
	PSE-Net	1.0G	12.6M	75.2%	92.0%	

Pruned Subnet Retraining. We train all pruned models from scratch. The pruned models are trained on 16 Tesla A100 GPUs with a batch size of 2048. For a fair comparison, the pruned ResNet50/MobileNetV2/VGG is trained for 120/450/100 total epochs. The initial learning rate for training pruned MobileNetV2 is first warming up from 0 to 0.8 within 20 epochs, then is reduced to 0 by the cosine scheduler. Other settings are the same as those of the supernet training.

4.2. Results on ImageNet Dataset

In this part, we compare our method with other multiple competing methods such as Roy et al. Miles and Mikolajczyk (2023), PEEL Hou et al. (2024), ARPruning Yuan et al. (2024), Tukan et al. Tukan et al. (2022), SANP Gao et al. (2023), DMCP Guo et al. (2020a), TAS Dong and Yang (2019), AutoSlim Yu and Huang (2019a), MetaPruning Liu et al. (2019), AMC He et al. (2018b), LEGR Chin et al. (2019), AutoPruner Luo and Wu (2020), SSS Huang and Wang (2018), and BCNet Su et al. (2021) on ImageNet dataset. Specifically, we search on the ResNet50 and MobileNetV2 with different FLOPs constraint, and report the accuracy on the validation dataset as Yu and Huang (2019a); Guo et al. (2020a). Following BCNet Su et al. (2021), we additionally take into account two naive baselines: (1) Uniform: we reduce the width of each layer by a constant factor to suit FLOPs budget requirements; (2) Random: we randomly pick 20 networks under the FLOPs restriction and train them for 50 epochs, and then continue training the

Table 2

Performance comparison of MobileNetV2 under ImageNet dataset. Performances are evaluated by using a single crop of 224×224. FLOPs is computed under the input resolution of 224×224. #Params denotes the number of parameters. Methods marked with “*” denote that reporting the results with knowledge distillation. † means the results reported in BCNet Su et al. (2021).

MobileNetV2						
FLOPs	Methods	FLOPs	#Params	Top-1	Top-5	
305M(1.5×)	Uniform [†]	305M	3.6M	72.7%	90.7%	
	Random [†]	305M	-	71.8%	90.2%	
	AutoSlim* Yu and Huang (2019a)	305M	5.7M	74.2%	-	
	BCNet Su et al. (2021) <i>cvpr21</i>	305M	4.8M	73.9%	91.5%	
	BCNet* Su et al. (2021) <i>cvpr21</i>	305M	4.8M	74.7%	92.2%	
	PEEL Hou et al. (2024) <i>pr24</i>	300M	-	74.2%	-	
	PEEL* Hou et al. (2024) <i>pr24</i>	300M	-	74.8%	-	
200M	PSE-Net	305M	4.1M	74.2%	91.7%	
	PSE-Net*	305M	4.1M	75.2%	92.4%	
	Uniform [†]	207M	2.7M	71.2%	89.6%	
	Random [†]	207M	-	70.5%	89.2%	
	AMC He et al. (2018b) <i>eccv18</i>	211M	2.3M	70.8%	-	
	AutoSlim* Yu and Huang (2019a)	207M	4.1M	73.0%	-	
	LEGR Chin et al. (2019)	210M	-	71.4%	-	
100M	MetaPruning Liu et al. (2019) <i>cvpr19</i>	217M	-	71.2%	-	
	BCNet Su et al. (2021) <i>cvpr21</i>	207M	3.1M	72.3%	90.4%	
	BCNet* Su et al. (2021) <i>cvpr21</i>	207M	3.1M	73.4%	91.2%	
	SANP Gao et al. (2023) <i>iccv23</i>	213M	3.6M	72.1%	90.4%	
	PEEL Hou et al. (2024) <i>pr24</i>	211M	-	73.0%	-	
	PEEL* Hou et al. (2024) <i>pr24</i>	211M	-	73.9%	-	
	PSE-Net	207M	3.0M	72.7%	90.9%	
100M	PSE-Net*	207M	3.0M	73.5%	91.4%	
	Uniform [†]	105M	1.5M	65.1%	89.6%	
	Random [†]	105M	-	63.9%	89.2%	
	MetaPruning Liu et al. (2019) <i>cvpr19</i>	105M	-	65.0%	-	
	BCNet Su et al. (2021) <i>cvpr21</i>	105M	2.3M	68.0%	89.1%	
	BCNet* Su et al. (2021) <i>cvpr21</i>	105M	2.3M	69.0%	89.9%	
	PEEL Hou et al. (2024) <i>pr24</i>	87M	-	66.0%	-	
PSE-Net	PEEL* Hou et al. (2024) <i>pr24</i>	87M	-	66.6%	-	
	PSE-Net	105M	1.8M	68.1%	89.5%	
PSE-Net*	PSE-Net*	105M	1.8M	69.4%	90.3%	

Table 3

Performance comparison of VGG16 on ImageNet dataset. FLOPs is computed under the input resolution of 224×224. #Params denotes the number of parameters.

	FLOPs	#Params	Top-1	Top-5
VGG Simonyan and Zisserman (2014)	15.53G	138.37M	73.74%	91.66%
PSE-Net	7.10G	120.99M	71.72%	90.62%
PSE-Net	10.49G	65.31M	71.45%	90.43%

network with the best performance and portray its final result alongside the results reported from BCNet Su et al. (2021). In our experiments, the original ResNet50/MobileNetV2 possesses 25.5M/3.5M parameters and 4.1G/300M FLOPs with 77.6%/72.6% Top-1 accuracy, respectively.

Comparison with SOTA Methods on ResNet50. As shown in Table 1, PSE-Net yields the best Top-1 accuracy on ImageNet by using ResNet50 He et al. (2016) as unpruned architecture. For example, comparing our 2G FLOPs ResNet50 to the original model, Top-1 accuracy reduces by only 0.3%. Compared with the current state-of-the-art BCNet Su et al. (2021), our 3G FLOPs and 2G FLOPs ResNet50 exceed it by 0.6% and 0.4% Top-1 accuracy. Besides, our 1G FLOPs ResNet50 achieves similar performance with BCNet under comparable FLOPs and parameters. Notably, PSE-Net is more efficient than BCNet in terms of supernet training, which is demonstrated in Section 4.3. Compared with AutoSlim Yu and Huang (2019a), PSE-Net under all FLOPs

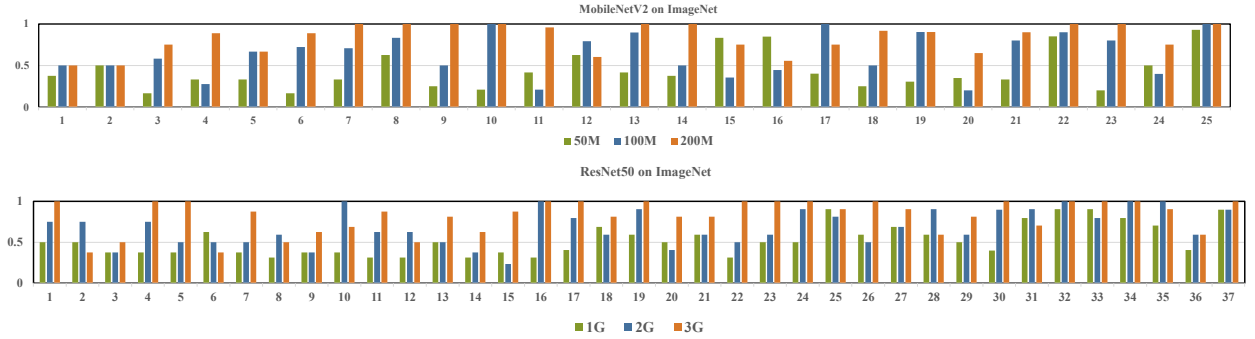


Figure 3: Visualization of the searched networks relative to different FLOPs. The abscissa represents the serial number of the convolutional layer. For each layer, the vertical axis represents the ratio of maintained channels to those of the original networks.

levels surpasses it by non-trivial margins, demonstrating the efficacy of simulating multiple subnets forward-backward in one round. Moreover, compared with the two vanilla baselines and other previous works, PSE-Net also exhibits predominant performances.

Comparison with SOTA Methods on MobileNetV2.

The pruned results for MobileNetV2 are reported in Table 2. Specifically, our 300M FLOPs PSE-Net/PSE-Net* reaches 74.2%/75.2% Top-1 accuracy, which outperforms the state-of-the-art BCNet/BCNet* Su et al. (2021) by 0.3%/0.5% with comparable FLOPs and a decrease of 0.7M parameters. Compared with AutoSlim* Yu and Huang (2019a), our 300M FLOPs PSE-Net* exceeds it by 1%, further demonstrating the superiority of PSE-Net. In addition, our 200M FLOPs PSE-Net achieves 72.7% Top-1 accuracy, which also exceeds BCNet Su et al. (2021), MetaPruning Liu et al. (2019), and LEGR Chin et al. (2019) by 0.4%, 1.5% and 1.3% respectively. Compared with BCNet* Su et al. (2021) and AutoSlim* Yu and Huang (2019a), our 200M FLOPs PSE-Net* also surpasses them by 0.1% and 0.5 respectively. Compared to the two vanilla baselines, Uniform and Random, our all FLOPs level MobileNetV2 significantly outperforms both.

VGG Results on ImageNet Dataset. The pruned results for VGG are reported in Table 3. Our 7G FLOPs pruned VGG obtains 71.72% top-1 accuracy while our 10G FLOPs pruned VGG derives 71.45% top-1 accuracy, which is induced by the parameters of 7G FLOPs pruned VGG significantly higher than those of 10G FLOPs pruned VGG.

Visualization. For intuitive comprehension, we visualize our searched PSE-Net under various FLOPs in Fig. 3. In addition, the maintained ratio of layer widths relative to the original models is displayed for clarification. Yet, the last few layers have a greater likelihood of being retained. This might be due to the fact that the last few layers are more sensitive to the classification performance, and hence, it can be securely maintained when the FLOPs are decreased, as the same phenomenon is observed in BCNet Su et al. (2021).

4.3. Effect and Efficiency Analysis of Parallel-subnets Training Algorithm

In this part, we compare the effect and efficiency of the parallel-subnets training algorithm with prior works by

leveraging ResNet50 as unpruned architecture. We construct ablation experiments as follows: (1) SPOS[‡]: we train the supernet by randomly sampling a subnet at each training iteration, which is also adopted by SPOS Guo et al. (2020b). (2) BCNet: at each training iteration, following Su et al. (2021), two bilaterally coupled subnets are sampled for supernet training, where the selected channel width sums up to the max channels in the same layer. (3) AutoSlim[‡]: we sample 4 subnets, i.e., the max subnet, the min subnet, and two random sampled subnets. Data is serially fed into the subnets and their gradients are accumulated for parameters updating. The sandwich rule is widely adopted in Yu and Huang (2019a); Yu et al. (2020); Wang, Li, Gong and Chandra (2021). For effect analysis, we train the supernet by 120 epochs by using 16 Tesla A100 GPUs following the training recipe of PSE-Net. For efficiency analysis, an AutoML-based pruning method typically involves three steps: Step1: Optimizing a supernet over a number of epochs to effectively derive a benchmark performance estimator; Step2: Iteratively evaluating the trained supernet and selectively reducing the channels with minimal accuracy drop on the validation set; and Step3: Obtaining the optimized channel configurations under various resource constraints and retraining these optimized pruning configurations. For Step3, all the methods share almost the same pipeline. For Step2, the main cost is incurred in evaluating accuracy on the validation set, we kept the number of channel configurations evaluated the same for fair comparison. In Step1, since different methods use different GPUs to training their supernet, we compare the number of executing forward-backward times, time cost at each training iteration and total training epochs. The iter_time is measured on a Tesla A100 GPU with input shape of data as (128, 3, 224, 224).

As shown in Table 4, the top-1 accuracy of ResNet50-1G/2G/3G searched by our method significantly outperforms those of the baseline (SPOS[‡]) by 1.0%/1.2%/1.2% with comparable iter_time cost, illustrating that the significance of our proposed parallel-subnets training algorithm for efficient and effective supernet training. Compared with BCNet Su et al. (2021), our pruned ResNet50-2G/3G also exceeds it by 0.4%/0.6% with 73% iter_time time cost and only 30% total time cost, further highlighting the supremacy

Table 4

Effect and efficiency analysis of parallel-subnets training algorithm. #Fw-Bw denotes that the number of executing forward-backward times at each training iteration. Iter_time means the time cost at each training iteration. \ddagger indicates the accuracy is reproduced by us using the same pipeline.

	#Fw-Bw	Iter_time	epochs	Top-1(1G/2G/3G)
SPOS [‡] Guo et al. (2020b)	1	169ms	120	74.2% / 76.1% / 76.7%
BCNet Su et al. (2021)	2	303ms	300	75.2% / 76.9% / 77.3%
AutoSlim [‡] Yu and Huang (2019a)	4	555ms	300	75.1% / 77.4% / 77.9%
Ours	1	221ms	120	75.2% / 77.3% / 77.9%

Table 5

The effect of our proposed parallel-subnets training algorithm. We adopt MobiNetV2 200M FLOPs for comparison.

	FLOPs (M)	#Params (M)	Top-1
EXP1	205	2.85	71.6%
EXP2	212	3.02	71.5%
EXP3	210	2.93	72.4%
EXP4	208	3.02	72.3%
PSE-Net	213	3.03	72.7%

of our presented parallel-subnets training algorithm. In addition, our method achieves equivalent performance with the naive serial training technique (i.e., sandwich rule) at a significantly lower expense in time costs (40% iter_time and 16% total time cost).

4.4. Ablation Study

Effect of Our Parallel-subnets Training Algorithm. In this part, we verify the efficacy of our proposed parallel-subnets training algorithm by using the MobileNetV2 as unpruned network. As illustrated in Section 4.1, we split the input into $n = 4$ parts and simulate multiple networks (one largest subnet and three random middle subnets) to execute forward-backward pass in one round at each training iteration. Thus, we explore the concrete form of simulating multiple subnets by our parallel-subnets training algorithm. Specifically, we implement the following ablation experiments: (1) EXP1: simulating four random middle subnets at each training iteration; (2) EXP2: simulating one smallest subnet and three random middle subnets at each training iteration; (3) EXP3: simulating one largest subnet, one smallest subnet and two random middle subnets at each training iteration. (4) EXP4: simulating one largest subnet and two random middle subnets at each training iteration. The results are summarized in Table 5. We observe that PSE-Net achieves higher performance compared with EXP1, EXP2, EXP3, and EXP4. Compared EXP3, EXP4, and PSE-Net with EXP1 and EXP2, we can find that the largest subnet has a dominant influence on the performance, than other types of subnets.

Efficiency of Search Space. As illustrated in Section 3.1, we partition the channels of each layer into K groups to reduce the search space. In this part, we search for the MobileNetV2 with various group sizes K under ImageNet dataset. As shown in Table 6, our method obtains the best performance at our default value $K = 20$. Besides,

Table 6

The accuracy performance of the 200M FLOPs searched PSE-Net under various group sizes K of the search space.

K	FLOPs (M)	#Params (M)	Top-1
4	207	2.9	71.9%
12	214	2.8	72.1%
20	213	3.0	72.7%
28	212	2.9	72.3%
36	209	3.0	72.6%

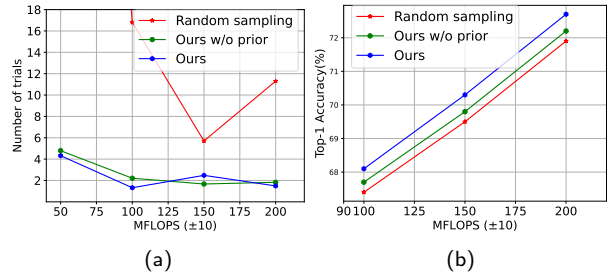


Figure 4: (a) The average number of trials to sample architectures under constraints. (b) Accuracy performance of the searched PSE-Net with different sampling methods.

we observe that when K is small, the performance of the searched network improves as K increases. This occurs because K influences the size of the search space \mathcal{A} , and a larger group size K results in a larger search space, enabling the searched PSE-Net to be closer to the ideal width. Moreover, performance tends to deteriorate when the group size is too large, indicating that the search space may be too broad for identifying the optimal width.

Effect of Prior-Distributed-Based Sampling Algorithm. Our prior-distributed-based sampling algorithm is employed in the search process to sample architectures under different FLOPs constraints. In this part, we conduct the following ablation experiments to validate the efficacy of our sampling algorithm: (1) Random sampling: randomly sampling a subnet during the evolutional search process; (2) Ours w/o quality prior information: without using subnet quality (training loss) prior information during sampling, which is also similar to Wang et al. (2021). We compare the average number of sampling trials for sampling the targeted architecture under the constraint, as illustrated in Fig. 4 (a). Due to the long-tail distribution of network architecture, we notice that random sampling poses a challenge to sample subnets that satisfy border resource limitations, whereas our sampling methods with/without quality prior information are both more effective. Moreover, as shown in Fig. 4 (b), the accuracy performance of subnets searched by our sampling method provides continuous exceptionalism over random sampling and our sampling method without quality prior information, further demonstrating the significance of the prior information of supernet training in assisting the search for the optimal subnet.

Effect of Training Supernet with Different Epochs. Our method is crucial for searching width as a fundamental

Table 7

Accuracy performance of the searched 200M FLOPs PSE-Net under various epochs for supernet training.

Epochs	FLOPs (M)	#Params (M)	Top-1
30	203	2.7	71.8%
60	205	2.8	72.4%
90	213	3.0	72.7%
120	208	3.0	72.5%
150	214	2.9	72.6%

Table 8

Performance of detection task with ResNet50 as the backbone under RetinaNet and Faster RCNN methods.

Methods	Original (4G)	BCNet (2G)	PSE-Net (2G)
RetinaNet Lin, Goyal, Girshick, He and Dollár (2017b)	36.4%	35.4%	35.9%
Faster RCNN Ren, He, Girshick and Sun (2015)	37.3%	36.3%	36.8%

Table 9

Performance of semantic segmentation task with ResNet50 as the backbone under Deeplabv3 method.

Method	Original (4G)	BCNet(2G)	PSE-Net (2G)
Deeplabv3 Chen, Papandreou, Schroff and Adam (2017)	78.58%	77.82	78.12%

performance estimator, which equips the network with the ability to interpolate the accuracy of unsampled subnets. In this part, we investigate how much effort should be devoted to supernet training to ensure the search performance. Thus, we train our approach with a variety of epochs and leverage the supernets to search MobileNetV2 with 200M FLOPs on the ImageNet dataset. The top-1 accuracies of the searched subnets are shown in Table 7. From Table 7, we can see that the top-1 accuracy of training 90 epochs is 0.9% better than that of training 30 epochs. As the number of epochs continues to increase, there is no significant increase in top1 accuracy. Thus, in this work, we train our PSE-Net 90 epochs in total.

4.5. Transferability to Downstream Tasks

Then, we applied the pruned PSE-Net to tasks of object detection and semantic segmentation based on frameworks MMDetection Chen, Wang, Pang, Cao, Xiong, Li, Sun, Feng, Liu, Xu, Zhang, Cheng, Zhu, Cheng, Zhao, Li, Lu, Zhu, Wu, Dai, Wang, Shi, Ouyang, Loy and Lin (2019) and MMSegmentation Contributors (2020), respectively.

Object Detection. In this part, we evaluate PSE-Net on object detection task. Experiments are performed using the COCO dataset, which includes 118K training images and 5K validation images of a whole of 80 classes. We take the searched 2G FLOPs ResNet50 subnets as the backbone under the two typical detection frameworks: RetinaNet Lin et al. (2017b) and Faster R-CNN Ren et al. (2015). Following the popular MMDetection Chen et al. (2019) toolbox, we train both RetinaNet and Faster R-CNN for 12 epochs, with a mini-batch of 16/16 and an initial learning rate of 0.01/0.02 for RetinaNet/Faster R-CNN. The learning rate is divided by 10 after 8 and 11 epochs. We employ SGD optimizer

with a weight decay of 1e-4. During the training and testing stages, the shorter side of input photos are shrunk to 800 pixels along the shorter dimension. The longer side will maintain the image ratio within 1333 pixels. In the training stage, we only leverage random horizontal flipping for data augmentation. We report the results in terms of AP in Table 8. PSE-Net (2G) surpasses the current state-of-the-art pruning algorithm BCNet Su et al. (2021) by 0.5% and 0.5%, respectively, in both the RetinaNet and Faster R-CNN frameworks, demonstrating its supremacy.

Semantic Segmentation. We also evaluate the searched 2G FLOPs ResNet50 on the semantic segmentation task with the Cityscapes dataset. The Cityscapes dataset is a large-scale urban street scene segmentation dataset. It contains high-resolution street scene images from 50 cities across the world, with a pixel-level annotation of 19 semantic classes, including vehicles, buildings, road surfaces, vegetation, pedestrians, cyclists, and more. We select Deeplabv3 Chen et al. (2017) as a basic method to validate our pruned 2G FLOPs ResNet50. The networks are trained for 40K iterations by applying SGD, with an initial learning rate of 0.01 and weight decay of 4e-5. We adopt the poly learning rate schedule with $\gamma=0.9$ and each mini-batch of 16. We resize and randomly crop images to 769×769 for training. During the testing stage, images are resized to the shorter side of 1025 pixels. We report mIoU of PSE-Net in single scale testing. The results are summarized in Table 9. We observe that PSE-Net(2G) achieves 78.12% mIoU, which surpasses the current state-of-the-art pruning algorithm BCNet(2G) than 0.3% and is slightly lower than the original model with a decrease of 2G FLOPs, further demonstrating the superiority of PSE-Net.

4.6. Latency of PSE-Net

Since there is a gap between FLOPs and the hardware latency, we compare the latency of PSE-Net with that of the baseline (the original ResNet50) and other state-of-the-art methods, as shown in Table 10. The latency of these methods are measured on a Tesla A100 GPU with input shape of data as (64, 3, 224, 224). PSE-Net surpasses the original ResNet50 model by 5.75/8.35/11.95 units under 3G/2G/1G FLOPs settings, respectively. Compared with DMCP, our 3G/2G/1G FLOPs ResNet50 models all achieve better performance. Compared with BCNet, our 3G/1G FLOPs ResNet50 models perform more efficiently on hardware, while the 2G FLOPs setting also achieves comparable result, further demonstrating the efficacy of PSE-Net.

5. Conclusion

In this work, we introduce PSE-Net, a novel parallel subnets estimator dedicated to efficient yet effective channel Pruning. PSE-Net is equipped with the proposed training algorithm, the parallel-subnets training algorithm. Under this algorithm, PSE-Net can simulate forward-backward of multiple sampled subnets in one round, improving the

Table 10

Latency of PSE-Net compared with the baseline and other state-of-the-art methods. To make the results reliable and stable, we warm up the networks and measure their latency multiple times and calculate their means.

	Original(4G)	3G	2G	1G
ResNet50 He et al. (2016)	25.50ms	-	-	-
DMCP Guo et al. (2020a)	-	23.05ms	20.05ms	14.45ms
BCNet Su et al. (2021)	-	22.35ms	17.05ms	15.05ms
PSE-Net	-	19.75ms	17.15ms	13.55ms

training efficiency of the supernet while arming the network with the capability of interpolating the accuracy of unsampled subnets. Over the trained PSE-Net, we devise a prior-distributed-based sampling algorithm to boost the performance of the classical evolutionary search. Such an algorithm employs the prior knowledge of supernet training to aid in the search for optimal subnets while addressing the difficulty of finding samples that satisfy resource limitations due to the long-tail distribution of network setup. Extensive experiments demonstrate PSE-Net outperforms previous state-of-the-art channel pruning methods on the ImageNet dataset and downstream tasks.

References

Camci, E., Gupta, M., Wu, M., Lin, J., 2022. Qlp: Deep q-learning for pruning deep neural networks. *IEEE Transactions on Circuits and Systems for Video Technology* 32, 6488–6501.

Chen, K., Wang, J., Pang, J., Cao, Y., Xiong, Y., Li, X., Sun, S., Feng, W., Liu, Z., Xu, J., Zhang, Z., Cheng, D., Zhu, C., Cheng, T., Zhao, Q., Li, B., Lu, X., Zhu, R., Wu, Y., Dai, J., Wang, J., Shi, J., Ouyang, W., Loy, C.C., Lin, D., 2019. MMDetection: Open mmlab detection toolbox and benchmark. *arXiv preprint arXiv:1906.07155*.

Chen, L.C., Papandreou, G., Schroff, F., Adam, H., 2017. Rethinking atrous convolution for semantic image segmentation. *arXiv preprint arXiv:1706.05587*.

Chen, Z., Liu, C., Yang, W., Li, K., Li, K., 2022. Lap: Latency-aware automated pruning with dynamic-based filter selection. *Neural Networks* 152, 407–418.

Chin, T.W., Ding, R., Zhang, C., Marculescu, D., 2019. Legr: Filter pruning via learned global ranking. *arXiv preprint arXiv:1904.12368* 85, 86.

Chu, X., Zhang, B., Xu, R., 2021. Fairnas: Rethinking evaluation fairness of weight sharing neural architecture search, in: *Proceedings of the IEEE/CVF International Conference on Computer Vision*, pp. 12239–12248.

Contributors, M., 2020. MMSegmentation: Openmmlab semantic segmentation toolbox and benchmark. <https://github.com/open-mmlab/mmsegmentation>.

Dong, X., Yang, Y., 2019. Network pruning via transformable architecture search. *Advances in Neural Information Processing Systems* 32.

Gao, S., Zhang, Z., Zhang, Y., Huang, F., Huang, H., 2023. Structural alignment for network pruning through partial regularization, in: *Proceedings of the IEEE/CVF International Conference on Computer Vision*, pp. 17402–17412.

Girshick, R., 2015. Fast r-cnn, in: *Proceedings of the IEEE international conference on computer vision*, pp. 1440–1448.

Guo, S., Wang, Y., Li, Q., Yan, J., 2020a. Dmcp: Differentiable markov channel pruning for neural networks, in: *Proceedings of the IEEE/CVF conference on computer vision and pattern recognition*, pp. 1539–1547.

Guo, Z., Zhang, X., Mu, H., Heng, W., Liu, Z., Wei, Y., Sun, J., 2020b. Single path one-shot neural architecture search with uniform sampling, in: *European Conference on Computer Vision*, Springer. pp. 544–560.

Han, S., Pool, J., Tran, J., Dally, W., 2015. Learning both weights and connections for efficient neural network. *Advances in neural information processing systems* 28.

He, K., Zhang, X., Ren, S., Sun, J., 2016. Deep residual learning for image recognition, in: *Proceedings of the IEEE conference on computer vision and pattern recognition*, pp. 770–778.

He, Y., Ding, Y., Liu, P., Zhu, L., Zhang, H., Yang, Y., 2020. Learning filter pruning criteria for deep convolutional neural networks acceleration, in: *Proceedings of the IEEE/CVF conference on computer vision and pattern recognition*, pp. 2009–2018.

He, Y., Kang, G., Dong, X., Fu, Y., Yang, Y., 2018a. Soft filter pruning for accelerating deep convolutional neural networks, in: *Proceedings of the 27th International Joint Conference on Artificial Intelligence*, pp. 2234–2240.

He, Y., Lin, J., Liu, Z., Wang, H., Li, L.J., Han, S., 2018b. Amc: Automl for model compression and acceleration on mobile devices, in: *Proceedings of the European conference on computer vision (ECCV)*, pp. 784–800.

He, Y., Liu, P., Wang, Z., Hu, Z., Yang, Y., 2019. Filter pruning via geometric median for deep convolutional neural networks acceleration, in: *Proceedings of the IEEE/CVF conference on computer vision and pattern recognition*, pp. 4340–4349.

Herath, S., Harandi, M., Porikli, F., 2017. Going deeper into action recognition: A survey. *Image and vision computing* 60, 4–21.

Hinton, G., Vinyals, O., Dean, J., et al., 2015. Distilling the knowledge in a neural network. *arXiv preprint arXiv:1503.02531* 2.

Hou, Y., Ma, Z., Liu, C., Wang, Z., Loy, C.C., 2024. Network pruning via resource reallocation. *Pattern Recognition* 145, 109886.

Hu, H., Peng, R., Tai, Y.W., Tang, C.K., 2016. Network trimming: A data-driven neuron pruning approach towards efficient deep architectures. *arXiv preprint arXiv:1607.03250*.

Huang, Z., Wang, N., 2018. Data-driven sparse structure selection for deep neural networks, in: *Proceedings of the European conference on computer vision (ECCV)*, pp. 304–320.

Kang, H.J., 2019. Accelerator-aware pruning for convolutional neural networks. *IEEE Transactions on Circuits and Systems for Video Technology* 30, 2093–2103.

Krizhevsky, A., Sutskever, I., Hinton, G.E., 2017. Imagenet classification with deep convolutional neural networks. *Communications of the ACM* 60, 84–90.

Li, H., Kadav, A., Durdanovic, I., Samet, H., Graf, H.P., . Pruning filters for efficient convnets, in: *International Conference on Learning Representations*.

Li, Y., Adamczewski, K., Li, W., Gu, S., Timofte, R., Van Gool, L., 2022. Revisiting random channel pruning for neural network compression, in: *Proceedings of the IEEE/CVF Conference on Computer Vision and Pattern Recognition*, pp. 191–201.

Lin, G., Milan, A., Shen, C., Reid, I., 2017a. Refinenet: Multi-path refinement networks for high-resolution semantic segmentation, in: *Proceedings of the IEEE conference on computer vision and pattern recognition*, pp. 1925–1934.

Lin, M., Ji, R., Wang, Y., Zhang, Y., Zhang, B., Tian, Y., Shao, L., 2020. Hrank: Filter pruning using high-rank feature map, in: *Proceedings of the IEEE/CVF conference on computer vision and pattern recognition*, pp. 1529–1538.

Lin, M., Ji, R., Zhang, Y., Zhang, B., Wu, Y., Tian, Y., 2021. Channel pruning via automatic structure search, in: *Proceedings of the Twenty-Ninth International Conference on International Joint Conferences on Artificial Intelligence*, pp. 673–679.

Lin, T.Y., Goyal, P., Girshick, R., He, K., Dollár, P., 2017b. Focal loss for dense object detection, in: *Proceedings of the IEEE international conference on computer vision*, pp. 2980–2988.

Liu, Z., Mu, H., Zhang, X., Guo, Z., Yang, X., Cheng, K.T., Sun, J., 2019. Metapruning: Meta learning for automatic neural network channel pruning, in: *Proceedings of the IEEE/CVF international conference on computer vision*, pp. 3296–3305.

Liu, Z., Sun, M., Zhou, T., Huang, G., Darrell, T., . Rethinking the value of network pruning, in: *International Conference on Learning Representations*.

Long, J., Shelhamer, E., Darrell, T., 2015. Fully convolutional networks for semantic segmentation, in: Proceedings of the IEEE conference on computer vision and pattern recognition, pp. 3431–3440.

Luo, J.H., Wu, J., 2020. Autopruner: An end-to-end trainable filter pruning method for efficient deep model inference. *Pattern Recognition* 107, 107461.

Luo, J.H., Wu, J., Lin, W., 2017. Thinet: A filter level pruning method for deep neural network compression, in: Proceedings of the IEEE international conference on computer vision, pp. 5058–5066.

Miles, R., Mikolajczyk, K., 2023. Reconstructing pruned filters using cheap spatial transformations, in: Proceedings of the IEEE/CVF International Conference on Computer Vision, pp. 1244–1252.

Molchanov, P., Tyree, S., Karras, T., Aila, T., Kautz, J., . Pruning convolutional neural networks for resource efficient inference, in: International Conference on Learning Representations.

Pan, J., Yang, S., Foo, L.G., Ke, Q., Rahmani, H., Fan, Z., Liu, J., 2023. Progressive channel-shrinking network. *IEEE Transactions on Multimedia*

Peng, H., Du, H., Yu, H., Li, Q., Liao, J., Fu, J., 2020. Cream of the crop: Distilling prioritized paths for one-shot neural architecture search. *Advances in Neural Information Processing Systems* 33, 17955–17964.

Rastegari, M., Ordonez, V., Redmon, J., Farhadi, A., 2016. Xnor-net: Imagenet classification using binary convolutional neural networks, in: Computer Vision–ECCV 2016: 14th European Conference, Amsterdam, The Netherlands, October 11–14, 2016, Proceedings, Part IV, Springer. pp. 525–542.

Redmon, J., Divvala, S., Girshick, R., Farhadi, A., 2016. You only look once: Unified, real-time object detection, in: Proceedings of the IEEE conference on computer vision and pattern recognition, pp. 779–788.

Ren, S., He, K., Girshick, R., Sun, J., 2015. Faster r-cnn: Towards real-time object detection with region proposal networks. *Advances in neural information processing systems* 28.

Sandler, M., Howard, A., Zhu, M., Zhmoginov, A., Chen, L.C., 2018. Mobilenetv2: Inverted residuals and linear bottlenecks, in: Proceedings of the IEEE conference on computer vision and pattern recognition, pp. 4510–4520.

Simonyan, K., Zisserman, A., 2014. Very deep convolutional networks for large-scale image recognition. *arXiv preprint arXiv:1409.1556* .

Su, X., You, S., Wang, F., Qian, C., Zhang, C., Xu, C., 2021. Bcnet: Searching for network width with bilaterally coupled network, in: Proceedings of the IEEE/CVF Conference on Computer Vision and Pattern Recognition, pp. 2175–2184.

Tukan, M., Mualem, L., Maalouf, A., 2022. Pruning neural networks via coresets and convex geometry: Towards no assumptions. *Advances in Neural Information Processing Systems* 35, 38003–38019.

Wang, D., Li, M., Gong, C., Chandra, V., 2021. Attentivenas: Improving neural architecture search via attentive sampling, in: Proceedings of the IEEE/CVF conference on computer vision and pattern recognition, pp. 6418–6427.

Wang, H., Schmid, C., 2013. Action recognition with improved trajectories, in: Proceedings of the IEEE international conference on computer vision, pp. 3551–3558.

Wang, P., Hu, Q., Fang, Z., Zhao, C., Cheng, J., 2017. Deepsearch: A fast image search framework for mobile devices. *ACM Transactions on Multimedia Computing, Communications, and Applications (TOMM)* 14, 1–22.

You, Z., Yan, K., Ye, J., Ma, M., Wang, P., 2019. Gate decorator: Global filter pruning method for accelerating deep convolutional neural networks. *Advances in neural information processing systems* 32.

Yu, J., Huang, T., 2019a. Autoslim: Towards one-shot architecture search for channel numbers. *arXiv preprint arXiv:1903.11728* .

Yu, J., Huang, T.S., 2019b. Universally slimmable networks and improved training techniques, in: Proceedings of the IEEE/CVF international conference on computer vision, pp. 1803–1811.

Yu, J., Jin, P., Liu, H., Bender, G., Kindermans, P.J., Tan, M., Huang, T., Song, X., Pang, R., Le, Q., 2020. Bignas: Scaling up neural architecture search with big single-stage models, in: European Conference on Computer Vision, Springer. pp. 702–717.

Yu, J., Yang, L., Xu, N., Yang, J., Huang, T., . Slimmable neural networks, in: International Conference on Learning Representations.

Yuan, T., Li, Z., Liu, B., Tang, Y., Liu, Y., 2024. Arpruning: An automatic channel pruning based on attention map ranking. *Neural Networks* , 106220.

Zhang, T., Ye, S., Zhang, K., Tang, J., Wen, W., Fardad, M., Wang, Y., 2018. A systematic dnn weight pruning framework using alternating direction method of multipliers, in: Proceedings of the European conference on computer vision (ECCV), pp. 184–199.

Zhao, C., Zhang, Y., Ni, B., 2023. Exploiting channel similarity for network pruning. *IEEE Transactions on Circuits and Systems for Video Technology* .